NATIONAL ADVISORY COMMITTEE FOR AERONAUTICS

TECHNICAL NOTE

No. 1525

STRESS AND DISTORTION MEASUREMENTS IN A 45° SWEPT BOX BEAM SUBJECTED TO BENDING AND TO TORSION

By George Zender and Charles Libove

Langley Memorial Aeronautical Laboratory
Langley Field, Va.

Washington
March 1948

NATIONAL ADVISORY COMMITTEE FOR AERONAUTICS

TECHNICAL NOTE NO. 1525

STRESS AND DISTORTION MEASUREMENTS IN A 45° SWEPT BOX BEAM SUBJECTED TO BENDING AND TO TORSION

By George Zender and Charles Libove

SUMMARY

An untapered aluminum-alloy box beam, representing the main structural component of a full-span, two-spar, 45° swept wing with a carry-through bay, was subjected to tip bending and twisting loads and its stresses and distortions were measured. Only symmetrical loading was considered and the stresses were kept below the proportional limit.

The investigation revealed that for bending the important effect of sweep was to cause a considerable build-up of normal stress and vertical shear stress in the rear spar (when considering the box beam as sweptback) near the fuselage. No such marked effect accompanied torsion. The stresses in the outer portions of the box, both in bending and in torsion, appeared to be unaffected by sweep and agreed fairly well with the stresses given by elementary beam formulas.

The investigation further revealed that the spar deflections of the swept box beam could be estimated approximately by analyzing the outer portions of the box beam as ordinary cantilevers and making adjustments for the flexibility of the inboard portion to which the cantilevers are joined.

INTRODUCTION

Present designs of aircraft for transonic speeds call for wings with large angles of sweep. In order to study the structural problems encountered in the design of swept wings a 45° swept box beam, shown in figures 1 and 2, was subjected to symmetrical tip loading and its stresses and distortions were measured. This paper gives the measured data and compares the stresses with those given by standard beam formulas and the distortions with those estimated on the basis of approximate calculations.

SYMBOLS

A	area enclosed by cross section, square inches
A_F	area of flange, square inches
E	Young's modulus of elasticity (10,500 ksi)
G	shear modulus of elasticity (4000 ksi)
I	geometric moment of inertia, inches^4
J	torsional stiffness constant, inches^4
K	shear-lag parameter
L	length, inches
M	bending moment, kip-inches
P	load, kips
Q	static moment, inches^3
T	torque, kip-inches
V	shear force, kips
X	longitudinal force, kips
a	depth of box beam, inches
b	width of box beam, inches
c	distance from neutral axis to any fiber, inches
h	depth of spar web, inches
l	length of triangular bay, inches
l_1, l_2	length of portions of carry-through bay, inches
s	perimeter of cross section, inches
t	thickness, inches
t_a	thickness of spar web, inches
t_b	thickness of cover sheet, inches

x	distance from origin, inches
y	deflection, inches
y_F	deflection of front spar, inches
y_R	deflection of rear spar, inches
w	warping displacement due to torque, inches
w_{hc}	warping displacement at cross section hc due to bending stresses, inches
α	rotation of cantilever portion due to flexibility of carry-through bay, radians
γ_W	shear strain of spar web
θ	rotation of cantilever portion due to flexibility of triangular bay, radians
Λ	angle of sweep, degrees
σ	longitudinal stress, ksi
ϕ	rotation of cross section due to torque, radians

TEST SPECIMEN

The pertinent details of the swept box beam are shown in figure 3. (Hereinafter the box beam is referred to as sweptback rather than swept, thus making it convenient to refer to the spars (or sidewalls) as "front" and "rear" without ambiguity.) The sweptback parts consisted of two boxes with their longitudinal axes at right angles, joined by and continuous with a short rectangular carry-through bay representing that part of the wing inside the fuselage. The material of the specimen was 24S-T aluminum alloy except for the bulkheads. The bulkheads consisted of rectangular steel sheets with a 90° bend at each edge, forming flanges for attachment to the spars and covers. Bulkheads 2, 3, 4, and 5 were $\frac{3}{32}$-inch thick, whereas all other bulkheads were $\frac{1}{8}$-inch thick.

The cover sheet and front spar web, but not the rear spar web, were spliced at the center line of the carry-through bay, and the stringers and spar flanges were spliced at the ends of the carry-through bay, as shown in figure 3. The front and rear spars were also reinforced at the ends of the carry-through bay where the box beam was supported.

METHOD OF TESTING

The setups for bending and twisting tests are shown in figures 1 and 2, respectively. The box was supported by steel rollers, with axes parallel to the direction of flight, at the four corners of the carry-through bay, and loads were applied at the tips of the box. (The bulkheads at the ends of the carry-through bay and the vertical reactions provided by the rollers taken together were assumed to represent the restraint that might be provided by a fuselage to the wing.) All loads were applied symmetrically at both tips by means of hand-operated winches. At each tip the load was transferred from the winch to a horizontal steel I-beam and then to the tip bulkhead in such a manner that the resultant load applied to the box was a vertical force acting through the center of the tip cross section for bending or a pure torque acting in the plane of the tip cross section for torsion.

Forces exerted by the winches were measured by means of dynamometers on which the smallest division was equivalent to approximately 10 pounds. Strains were measured only on the right half of the box beam by means of Tuckerman optical strain gages. A 2-inch gage length (smallest division, 0.000004 in./in.) was used for the measurement of all stringer strains; strains at a 45° angle to the spar-web center lines, used to determine shear stresses, were also measured with a 2-inch gage length (smallest division, 0.000002 in./in.). A 1-inch gage length (smallest division, 0.000004 in./in.) was used to obtain all other strains. Stringer and flange strains were converted to stresses using a value of $E = 10{,}500$ ksi; shear stresses were obtained from shear strains using a value of $G = 4000$ ksi. Spar deflections were measured by means of dial gages along the top flanges of the spars. The smallest division of these gages was equivalent to 0.001 inch in the bending tests and 0.0001 inch in the torsion tests.

RESULTS

Stresses due to bending.- The normal stresses in the stringers and flanges due to tip bending loads of 2.5 kips are shown in figure 4 and are compared with the stresses given by the formula $\frac{Mc}{I}$ of elementary beam theory, shown by means of dashed lines. The top-cover and spar shear stresses due to the same bending loads are shown in figure 5 and are compared with the stresses $\frac{VQ}{It}$ of elementary beam theory. The dotted parts of the stress curves in figures 4 and 5 in the inboard region of the rear spar are extrapolations representing the stresses that would exist if there were no reinforcement of the spar where it entered the carry-through bay.

Stresses due to torsion.- The shear stresses in the top cover and spar webs due to tip twisting moments of 43.42 kip-inches are given in figure 6 and are compared with the stresses $\frac{T}{2At}$ of ordinary shell theory. The stringer stresses developed by the same twisting moments are plotted in figure 7. The stringer stresses near the center line of the box beam in figure 7 are compared with the $\frac{Mc}{I}$-stress due to the component of the tip torque which produces bending of the carry-through bay.

Distortions due to bending.- The measured spar deflections due to tip loads of 2.5 kips are given in figure 8(a) and are compared with computed spar deflections shown by means of dashed curves. The computed deflection curves were obtained by assuming the beam to be clamped as a cantilever at bulkhead 6 and superimposing on the cantilever deflections the deflections due to the flexibility of the inner portion of the beam. A detailed description of these computations is contained in appendix A.

The measured and computed spar deflections shown in figure 8(a) were used to calculate the rotations (in their own planes) of cross sections perpendicular to the spars and cross sections parallel to the direction of flight. These cross-sectional rotations are shown in figure 8(b).

Distortions due to torsion.- The measured spar deflections due to tip twisting moments of 43.42 kip-inches are given in figure 9(a) and are compared with computed spar deflections, shown by means of dashed curves, obtained by applying ordinary torsion theory $\left(\frac{d\phi}{dx} = \frac{T}{GJ}\right)$ to the outer portion of the beam and then superimposing rigid-body translations and rotations due to the flexibility of the inner portion of the beam. The details of these computations are in appendix B.

The measured and computed spar deflections shown in figure 9(a) were used to calculate the cross-sectional rotations shown in figure 9(b).

DISCUSSION

Stresses due to bending.- The comparisons of experimental and computed results in figures 4 and 5 reveal that the stresses in the outer portions of the sweptback box beam, between the tip and a cross section about one chord length from bulkhead 6, are substantially the same as those given by elementary beam theory. Only the remaining portion of the box beam appears to be appreciably affected by sweepback and shear-lag effects.

The important effect of sweepback, as indicated in figures 4 and 5, is to cause an increase of normal stress and vertical shear in the rear spar immediately outboard of bulkhead 6 and a corresponding relief of stress in the front spar outboard of bulkhead 6. The normal stress in the rear spar outboard of bulkhead 6, extrapolated to eliminate the effect of local reinforcement, was 1.40 times the $\frac{Mc}{I}$-stress and the vertical shear stress, also extrapolated, was 1.33 times the vertical shear stress at the tip.

The build-up of stress in the rear spar near the carry-through bay can be explained qualitatively as follows: If the elastic restraint provided by the portion of the box beam inboard of bulkhead 6 were symmetrical, the stress distribution in the portion of the box outboard of bulkhead 6 would be as shown in figure 10(a). Actually, because of the triangular bay between bulkheads 6 and 8, more restraint is offered to the rear spar than to the front spar, and as a result the front spar rotates more in its own plane at bulkhead 6 than does the rear spar. The result is a warping of the cross section at bulkhead 6. Such a warping can be produced by means of a self-equilibrating antisymmetrical stress distribution applied to the portion outboard of bulkhead 6 as shown in figure 10(b). By the principle of superposition, the stress distribution of that portion of the sweptback box beam outboard of bulkhead 6 can be obtained by superimposing the stress distributions shown in figures 10(a) and 10(b). The resulting stress distribution is shown in figure 10(c) and is seen to be in good qualitative agreement, as far as the main characteristics are concerned, with the measured stress distributions outboard of bulkhead 6 shown in figures 4 and 5.

Calculations made for the box beam described herein and for a small Plexiglas box beam, similarly constructed and similarly loaded but having a solid carry-through bay clamped between two support blocks, indicate that the shear-lag part of the stress distribution at bulkhead 6 (fig. 10(a)) can be estimated by replacing the triangular bay by a rectangular bay clamped at its inboard end, with a length equal to 15 percent of the length of the front spar of the triangular bay, and making a conventional shear-lag calculation (reference 1) for the resulting cantilever box beam. The unknown magnitude of the torsion-bending part of the stress distribution (fig. 10(b)) could be estimated by applying the principle that the warping of the cross section at bulkhead 6 due to the stresses in figures 10(a) and 10(b), when the cross section is considered part of the inner portion (made up of the triangular and carry-through bays), must be the same as the warping when the cross section is considered part of the cantilever outer portion (shown in fig. 10). Such estimates would be necessarily crude because no theoretical data exist on the response of the inner portion to the stress distributions

shown in figures 10(a) and 10(b), although the response of the outer portion can be calculated from existing formulas (reference 2).

Stresses due to torsion.- The comparisons in figure 6 reveal that the top-cover and spar shear stresses due to tip twisting moments are substantially the same as those given by the elementary formula $\frac{T}{2At}$ (for torsion with constant rate of twist) in the outer portion of the beam, extending from the tip to a cross section about one chord length from bulkhead 6. From this cross section inboard to bulkhead 6 the cover and spar shears change slightly from their elementary values as a result of the restraint against cross-sectional warping provided by the triangular bay. This restraint against warping produces longitudinal stringer stresses (fig. 7) about half the magnitude of the shear stress $\frac{T}{2At}$ at bulkhead 6. From bulkhead 6 toward bulkhead 8 in the triangular bay both the cover and spar shears show a marked decrease.

Calculations show that, for the purpose of estimating the cover and spar shears and the bending stresses due to torsion just outboard of bulkhead 6, the triangular bay may be replaced by a rectangular bay of half the length clamped at its inboard end. The resulting structure is an ordinary cantilever box beam and the theory and formulas of reference 2 may be applied.

Distortions due to bending.- The reasonably good agreement between the theoretical and experimental spar deflections in figure 8(a) indicates the correctness of the basic assumption used in appendix A in estimating the spar deflections. This assumption is that as far as bending deflections are concerned the sweptback box beam behaves essentially as an ordinary cantilever from bulkhead 6 out, with displacements due to the flexibility of the carry-through bay and the triangular bay superimposed on the cantilever distortions.

The comparisons in figure 8(b) between the measured cross-sectional rotations and those deduced from the calculated spar deflections of figure 8(a) indicate that the calculated spar deflections are not accurate enough to use for the purpose of obtaining cross-sectional rotations, particularly rotations measured perpendicular to the spars. According to the assumptions used in calculating spar deflections in appendix A, rotations in their own planes of cross sections perpendicular to the spars can arise only from the bending of the carry-through bay. These rotations are given by the horizontal dashed curve in figure 8(b). The disagreement between this curve and the measured cross-sectional rotations is the result of an indeterminate amount of bending of bulkhead 6 in its own plane as well as the rate of twist caused by the warping of the cross section at bulkhead 6.

In order to check the approximate theory for calculating spar deflections, the bending test was repeated on a small Plexiglas model of construction similar to that of the large model but having a solid carry-through bay clamped between two support blocks. The same methods were used to calculate the spar deflections as were used for the large model, and the agreement between theory and experiment for the Plexiglas wing was as good as that obtained for the metal wing.

Distortions due to torsion.- Figure 9 indicates fair agreement between the experimental distortions and those calculated in appendix B. The torsion test was repeated on the small Plexiglas model mentioned in the previous section and the agreement between the experimental and calculated results was of the same order as that obtained for the large box beam.

CONCLUSIONS

The following conclusions apply to an untapered, aluminum-alloy, 45° sweptback box beam of the type for which test results are reported in this paper. The box beam was constructed to represent the main structural component of a full-span, two-spar, 45° swept wing with a rectangular carry-through bay and with ribs placed perpendicular to the spars. The conclusions are based on tests in which the loading was applied symmetrically with respect to the carry-through bay and consisted of vertical forces (bending loads) and torques (twisting loads) applied in the planes of the two tip cross sections. A cross section should be understood to mean a section cut by a plane perpendicular to the spars or side walls.

1. The stress phenomena peculiar to sweepback are confined to that portion of the box beam in and near the fuselage. The stresses in the outer portion of the box beam tested, extending from the tip to a cross section approximately one chord length from the last complete inboard cross section, were given with reasonable accuracy by elementary formulas for bending and torsion of beams.

2. The main effect of sweepback on the stresses due to bending loads is to produce a concentration of normal stress and vertical shear in the rear spar at the cross section immediately outboard of the carry-through bay, whereas the normal stress and vertical shear in the front spar at this cross section are relieved.

3. The most marked feature of the stresses due to torque loads is an appreciable decrease in the shear stresses in the covers and front spar in that portion of the box beam near the fuselage.

4. The spar deflections of the sweptback box beam can be estimated approximately by considering the outboard portions to be cantilevers and superimposing on the cantilever distortions rigid-body movements due to the flexibility of the inboard region to which the cantilevers are attached.

Langley Memorial Aeronautical Laboratory
National Advisory Committee for Aeronautics
Langley Field, Va., December 12, 1947

APPENDIX A

CALCULATIONS FOR DISTORTIONS IN BENDING

The theoretical spar deflections plotted in figure 8(a) are the sum of four separately calculated deflections.

The first of the component deflections are those obtained by assuming the portion of the beam outboard of bulkhead 6 (see accompanying sketch) to be clamped as a cantilever at bulkhead 6 and applying elementary bending theory to calculate its deflections.

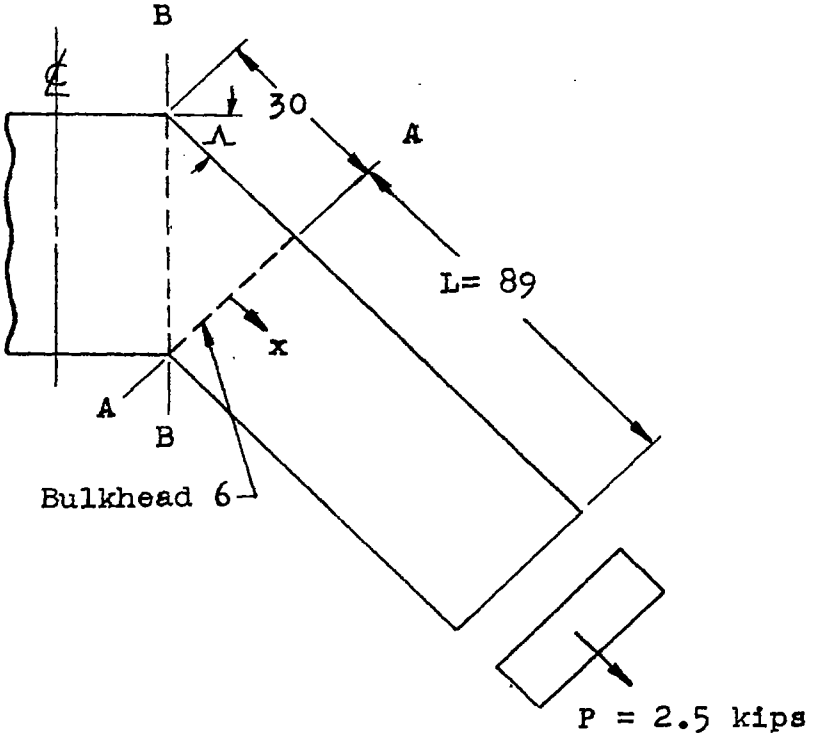

This assumption gives the following deflections y_F and y_R for the front and rear spars, respectively:

$$y_F = y_R = \frac{PL^3}{EI}\left[\frac{1}{2}\left(\frac{x}{L}\right)^2 - \frac{1}{6}\left(\frac{x}{L}\right)^3\right]$$

$$= \frac{2.5(89)^3}{10500(90.2)}\left[\frac{1}{2}\left(\frac{x}{89}\right)^2 - \frac{1}{6}\left(\frac{x}{89}\right)^3\right]$$

$$= 0.440x^2(267 - x)10^{-6} \text{ inches} \qquad (A1)$$

The second group of deflections comprises those due to shear in the spar webs, with the beam still assumed clamped as a cantilever at bulkhead 6. The spar deflections due to shear are calculated by assuming the vertical shear to be uniformly distributed in the spar webs (of depth h and thickness t_a) and calculating the resulting shear strain γ_w. For the symmetrical cross-section beam considered in the preceding paragraph, the shears are equal in the two spars and the spar deflections due to shear can be written as

$$y_F = y_R = \gamma_w x$$

$$= \frac{P}{2ht_aG} x$$

$$= \frac{2.5x}{2(7)(0.078)(4000)}$$

$$= 0.000572x \qquad \text{(A2)}$$

The third group of spar deflections are those due to the flexibility of the triangular bay, which is assumed to contribute a rotation θ to the cantilever about axis A-A. The magnitude of this rotation θ is calculated approximately by assuming the rotation to be the same as that which would be produced at the end of a rectangular bay of length equal to the average length of the triangular bay, if the rectangular bay were clamped at one end, the known bending moment at bulkhead 6 were applied at the other end, and plane sections were assumed to remain plane. The following sketch shows the rectangular bay in plan and elevation:

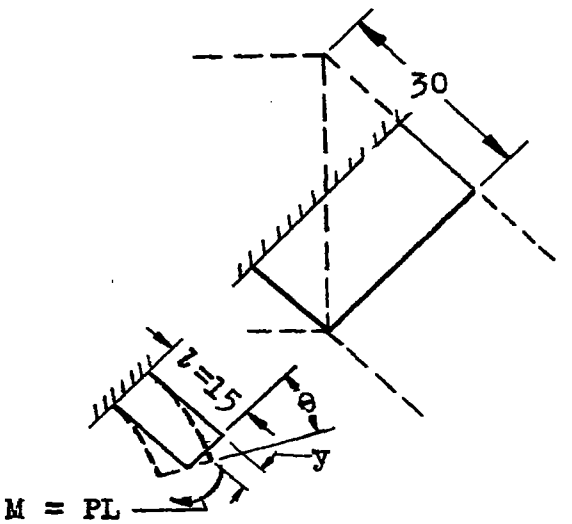

From elementary beam theory,

$$\theta = \frac{Ml}{EI}$$

$$= \frac{PLl}{EI}$$

$$= \frac{2.5(89)(15)}{10500(90.2)}$$

$$= 0.00353 \text{ radian}$$

The spar deflections produced by the rigid-body rotation θ about axis A–A are simply

$$y_F = y_R = \theta x = 0.00353x \qquad (A3)$$

Equation (A3) can be expected to overestimate somewhat the effect of the flexibility of the triangular bay, inasmuch as the bending moment M is not uniformly distributed over the chord but is concentrated near the rear spar (see stresses on fig. 4) where the shortness of the triangular bay reduces its effectiveness in permitting the cantilever to rotate. The flexibility of the rectangular substitute bay also contributes to the outboard portion of the box a small deflection (y on the sketch) which is neglected.

The last component of the total spar deflections is that due to the flexibility of the carry-through bay, which is assumed to contribute to the cantilever a rotation α about axis B–B (see first sketch of appendix A). The carry-through bay is shown in plan and elevation in the following sketch and the cross-sectional moments of inertia I_1 and I_2 in the spliced and unspliced portions, respectively, are indicated. The moment M is the moment about axis B–B of the known external loading on half the beam; that is, $M = P(L + 15) \cos \Lambda$.

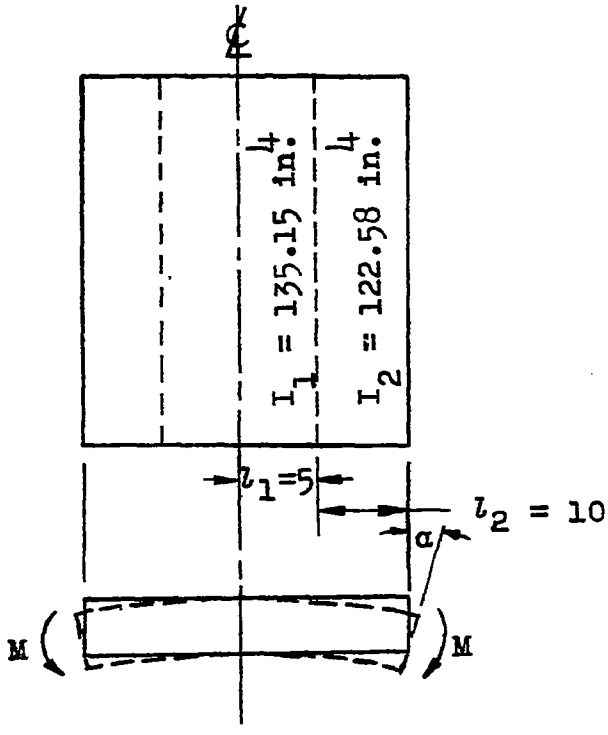

Again, by applying elementary beam theory, the rigid-body rotation α can be calculated as

$$\alpha = \frac{Ml_1}{EI_1} + \frac{Ml_2}{EI_2}$$

$$= \frac{M}{E}\left(\frac{l_1}{I_1} + \frac{l_2}{I_2}\right)$$

$$= \frac{P(L + 15)\cos\Lambda}{E}\left(\frac{l_1}{I_1} + \frac{l_2}{I_2}\right)$$

$$= \frac{2.5(104)(0.707)}{10500}\left(\frac{5}{135.15} + \frac{10}{122.58}\right)$$

$$= 0.00206 \text{ radian}$$

The spar deflections, produced by the rotation α of the cantilever about axis B–B, are

$$\left.\begin{aligned} y_F &= \alpha(x + 30)\cos\Lambda \\ &= 0.00208(x + 30)(0.707) \\ &= 0.00147(x + 30) \\ \\ y_R &= \alpha x \cos\Lambda \\ &= 0.00147x \end{aligned}\right\} \qquad (A4)$$

The total spar deflections are obtained by adding the individual spar deflections as calculated by equations (A1) to (A4). The calculated individual deflections and the total deflections for several stations along the spars are listed in the following table:

Type of deflection (deflection measured in in.) (a)	Spar	Station, x (in.)					
		0	20	40	60	80	100
Cantilever deflection (equation (A1))	Front	0	0.0435	0.1598	0.3278	0.5265	0.7345
	Rear	0	.0435	.1598	.3278	.5265	.7345
Deflection due to spar shear (equation (A2))	Front	0	.0114	.0229	.0343	.0458	.0572
	Rear	0	.0114	.0229	.0343	.0458	.0572
Deflection due to flexibility of triangular bay (equation (A3))	Front	0	.0706	.1412	.2118	.2824	.3530
	Rear	0	.0706	.1412	.2118	.2824	.3530
Deflection due to flexibility of carry–through bay (equation (A4))	Front	0.0441	.0735	.1029	.1323	.1617	.1911
	Rear	0	.0294	.0588	.0882	.1176	.1470
Total deflection	Front	0.0441	.1990	.4268	.7062	1.0164	1.3358
	Rear	0	.1549	.3827	.6621	.9723	1.2917

[a]Positive deflection downward.

(Note that the station $x = 100$ is off the spars, but its deflections were calculated for convenience in plotting.) The total calculated deflections are plotted in figure 8(a).

Rotations in their own planes of cross sections perpendicular to the spars result only from the flexibility of the carry-through bay, according to the assumptions made. These rotations are constant along the span and can be calculated by dividing the difference between front and rear spar deflections at any station by the width of the box; therefore, the rotation is $\frac{0.0441}{30} = 0.00147$ radian. This value is plotted as the horizontal dashed line in figure 8(b).

APPENDIX B

CALCULATIONS FOR DISTORTIONS IN TORSION

Initially the calculations for distortions in torsion are performed on the assumption that the carry-through bay is rigid. The flexibility of the carry-through bay is taken into account later by superimposing a rotation about axis B-B (see accompanying sketch) upon that portion of the beam outboard of bulkhead 6.

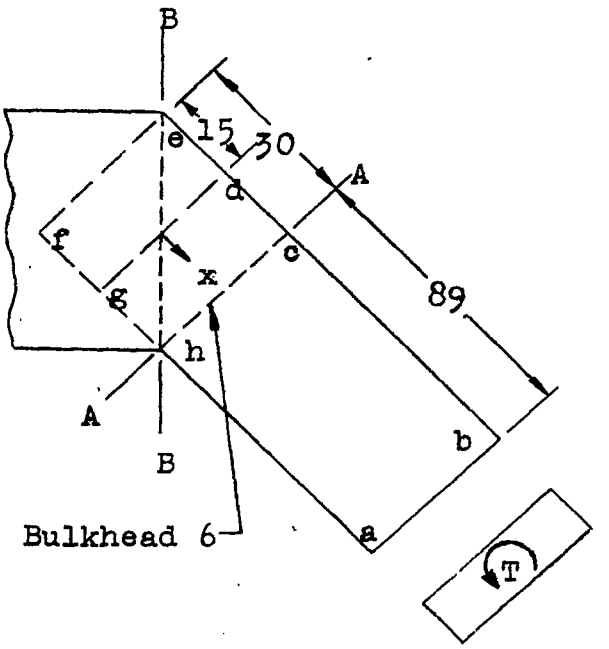

Tip torque, T = 43.42 kip-in.

The experimental results indicate that if the effect of the bending of the carry-through bay is subtracted from the twist, the rate of change of the remaining twist $\frac{d\phi}{dx}$ for cross sections perpendicular to the spars is in good agreement with the elementary formula

$$\frac{d\phi}{dx} = \frac{T}{GJ}$$

where

$$J = \frac{4A^2}{\oint \frac{ds}{t}}$$

The value of J is calculated as

$$J = \frac{4(7.05 \times 29.58)^2}{2\left(\frac{7.05}{0.078} + \frac{29.58}{0.050}\right)}$$

$$= 127.4 \text{ inches}^4$$

The experiments further indicate that the twist itself is obtained approximately by integrating the expression for $\frac{d\phi}{dx}$ and imposing the boundary condition $\phi = 0$ at $x = 0$, provided the origin for measurement of x is as shown in the sketch. Therefore,

$$\phi = \frac{Tx}{GJ}$$

$$= \frac{43.42x}{4000(127.4)}$$

$$= 0.000085x \text{ radian}$$

where x is in inches. The front and rear spar deflections due to ϕ are

$$\left.\begin{aligned} y_F &= -\frac{\phi b}{2} \\ &= -0.000085\left(\frac{30}{2}\right)x \\ &= -0.001278x \\ y_R &= \frac{\phi b}{2} \\ &= 0.001278x \end{aligned}\right\} \quad \text{(B1)}$$

Equations (B1) give deflections of 0.01917 inch in the front spar at $x = -15$ inches and in the rear spar at $x = 15$ inches. But $x = -15$ inches in the front spar and $x = 15$ inches in the rear spar correspond to the supports, the deflections of which must be zero. A vertical rigid-body translation is therefore imposed so as to eliminate the deflections at the supports. The front and rear spar deflections due to this rigid-body translation are

$$y_F = y_R = -0.01917 \text{ inch} \qquad (B2)$$

The spar deflections have thus far been calculated on the assumption that the central axis of the beam remains horizontal. The continuity between the cantilever portion and the triangular portion of the box beam will be shown to require a rigid-body rotation of the cantilever portion about axis A-A (see sketch in first paragraph).

First, the warping of the cross section at bulkhead 6 (cross section hc in the sketch) must be calculated. The carry-through-bay normal stress distribution in figure 7 is essentially constant; such a distribution indicates a rotation but no warping of cross section eh. Since the rotation of cross section eh causes only a rigid-body rotation of the outer portion, it does not affect the warping of cross section hc. For purposes of calculating the warping of cross section hc, the triangular bay may therefore be assumed to be clamped where it joins the carry-through bay. A plausible assumption is, furthermore, that the warping of cross section hc in the skew cantilever abeh will be approximately the same as the warping of cross section hc in the ordinary cantilever abdg clamped at cross section dg.

The warping of cross section hc in cantilever abdg can be calculated by applying formulas of reference 2. The box beam is first idealized in the usual manner into the four-element box for which a cross section is shown in the accompanying sketch.

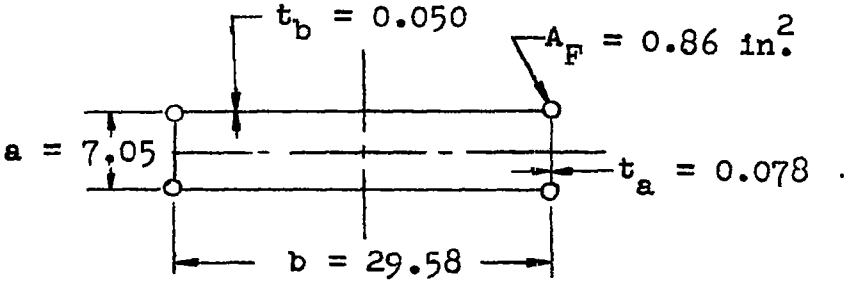

In order to simplify the calculations, the bulkheads or ribs are assumed infinitely close. If no restraint against warping existed (that is, no longitudinal stresses developed at the corners), then all cross sections would warp (that is, each corner of the cross section would move longitudinally) an amount w given by equation (21) of reference 2 as

$$w = \frac{T}{8Gba}\left(\frac{b}{t_b} - \frac{a}{t_a}\right)$$

where the sign conventions are those of reference 2. Then,

$$w = \frac{-43.42}{8(4000)(29.58)(7.05)}\left(\frac{29.58}{0.050} - \frac{7.05}{0.078}\right)$$

$$= -0.00326 \text{ inch}$$

Bending stresses due to torsion are developed at cross section gd of sufficient magnitude to eliminate the warping of cross section gd. Or, from equations (25), (30), and (15) of reference 2

$$X = wKA_F E$$

$$= w\sqrt{\frac{8GA_F E}{\frac{b}{t_b} + \frac{a}{t_a}}}$$

$$= -0.00326\sqrt{\frac{8(4000)(0.86)(10500)}{\frac{29.58}{0.050} + \frac{7.05}{0.078}}}$$

$$= -2.125 \text{ kips}$$

The direction of the X-forces at the root are shown in the following sketch:

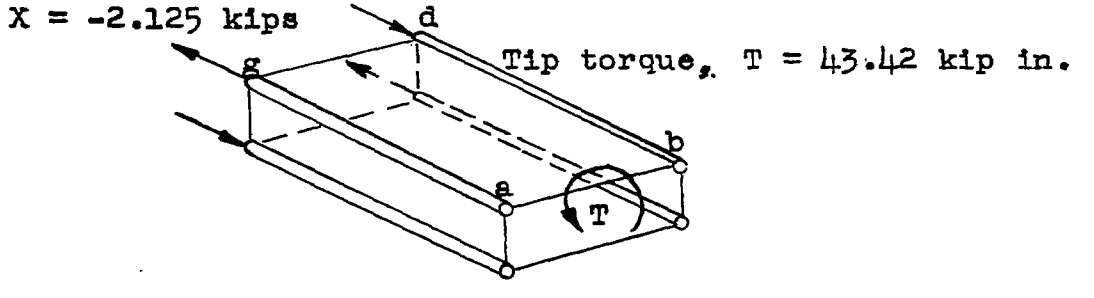

If abgd is regarded as one bay with infinitely close bulkheads, equation (13) of reference 2 can be used to calculate the bending stresses due to torsion at cross section hc. After revision in accordance with the notation used in the sketch accompanying the first paragraph of this appendix, equation (13) of reference 2 gives the following expression for the bending forces X_{hc} at cross section hc:

$$X_{hc} = \sigma A_F$$

$$= X \frac{\sinh (89K)}{\sinh (104K)}$$

where

$$K = \sqrt{\frac{8G}{A_F E\left(\frac{b}{t_b} + \frac{a}{t_a}\right)}}$$

$$= \sqrt{\frac{8(4000)}{0.86(10500)(682)}}$$

$$= 0.0721$$

Therefore,

$$X_{hc} = -2.125 \frac{\sinh 6.42}{\sinh 7.50}$$

$$= -2.125 \frac{307.01}{904.02}$$

$$= -0.722 \text{ kip}$$

Now if the portion abdg is considered a long bay, the warping of cross section hc produced by the forces X_{hc} is calculated from equations (25), (30), and (15) of reference 2 as

$$w_{hc} = \frac{-X_{hc}}{KA_F E}$$

$$= \frac{0.722}{0.0721(0.86)(10500)}$$

$$= 0.00111 \text{ inch}$$

The total warping of cross section hc is the warping w due to torque, calculated previously, plus the warping w_{hc} due to the bending stresses developed at cross section hc by the clamping at the root. The total warping is therefore $-0.00326 + 0.00111$ or -0.00215 inch. If the central axis of the beam remains horizontal, the warping of cross section hc implies that a vertical line at h in the rear spar ha must rotate through an angle of $\frac{0.00215}{7.05/2}$ (where 7.05/2 is one-half the depth of the idealized beam) or 0.00061 radian in the plane of the spar, clockwise as viewed from the rear. This implication violates continuity between the rear spar and the carry-through bay (still assumed rigid). Continuity can be reestablished by rotating portion abch upward through an angle of 0.00061 radian about axis A-A. This rigid-body rotation produces the spar deflections

$$y_F = y_R = -0.00061(x - 15) \text{ inches} \qquad (B3)$$

for $x \geq 15$.

The flexibility of the carry-through bay must still be taken into account. Its effect will be a rigid-body rotation about axis B-B, calculated by application of elementary beam theory to the carry-through bay just as was done in appendix A. The essentially constant stress distribution in the carry-through bay, as indicated in figure 7, makes such a calculation more justifiable in the present case than it was in the bending case. The equation for the rotation α in appendix A may be used here with M replaced by

$$-T \sin \Lambda = -(43.42)(0.707)$$

$$= -30.7 \text{ inch-kips}$$

with the result that $\alpha = -0.000169$ radian. The corresponding front and rear spar deflections are, respectively,

$$\left.\begin{aligned} y_F &= -\alpha(x + 15)\cos\Lambda \\ &= -0.000169(x + 15)(0.707) \\ &= -0.0001195(x + 15) \\ \\ y_R &= -\alpha(x - 15)\cos\Lambda \\ &= -0.0001195(x - 15) \end{aligned}\right\} \quad \text{(B4)}$$

The total spar deflections are obtained by superimposing the component spar deflections given by equations (B1) to (B4). These component deflections and the total deflections are listed in the following table for two stations along the spars.

Type of deflection (deflection measured in in.) (a)	Spar	Station, x (in.)	
		20	100
Deflection due to elementary twisting (equation (B1))	Front	-0.0256	-0.1278
	Rear	.0256	.1278
Rigid-body translation to give zero deflection at supports (equation (B2))	Front	-.0192	-.0192
	Rear	-.0192	-.0192
Deflection to establish continuity with triangular bay (equation (B3))	Front	-.0031	-.0519
	Rear	-.0031	-.0519
Deflection due to flexibility of carry-through bay (equation (B4))	Front	-.0042	-.0137
	Rear	-.0006	-.0101
Total deflection	Front	-.0521	-.2126
	Rear	.0027	.0466

[a]Positive deflection downward.

Since the equations for the total spar deflections are linear in x, straight lines may be drawn between the total deflections tabulated for stations 20 and 100 to obtain the total deflections at intermediate stations. The total deflections are plotted in figure 9(a).

REFERENCES

1. Kuhn, Paul: A Recurrence Formula for Shear-Lag Problems. NACA TN No. 739, 1939.

2. Kuhn, Paul: A Method of Calculating Bending Stresses Due to Torsion. NACA ARR, Dec. 1942.

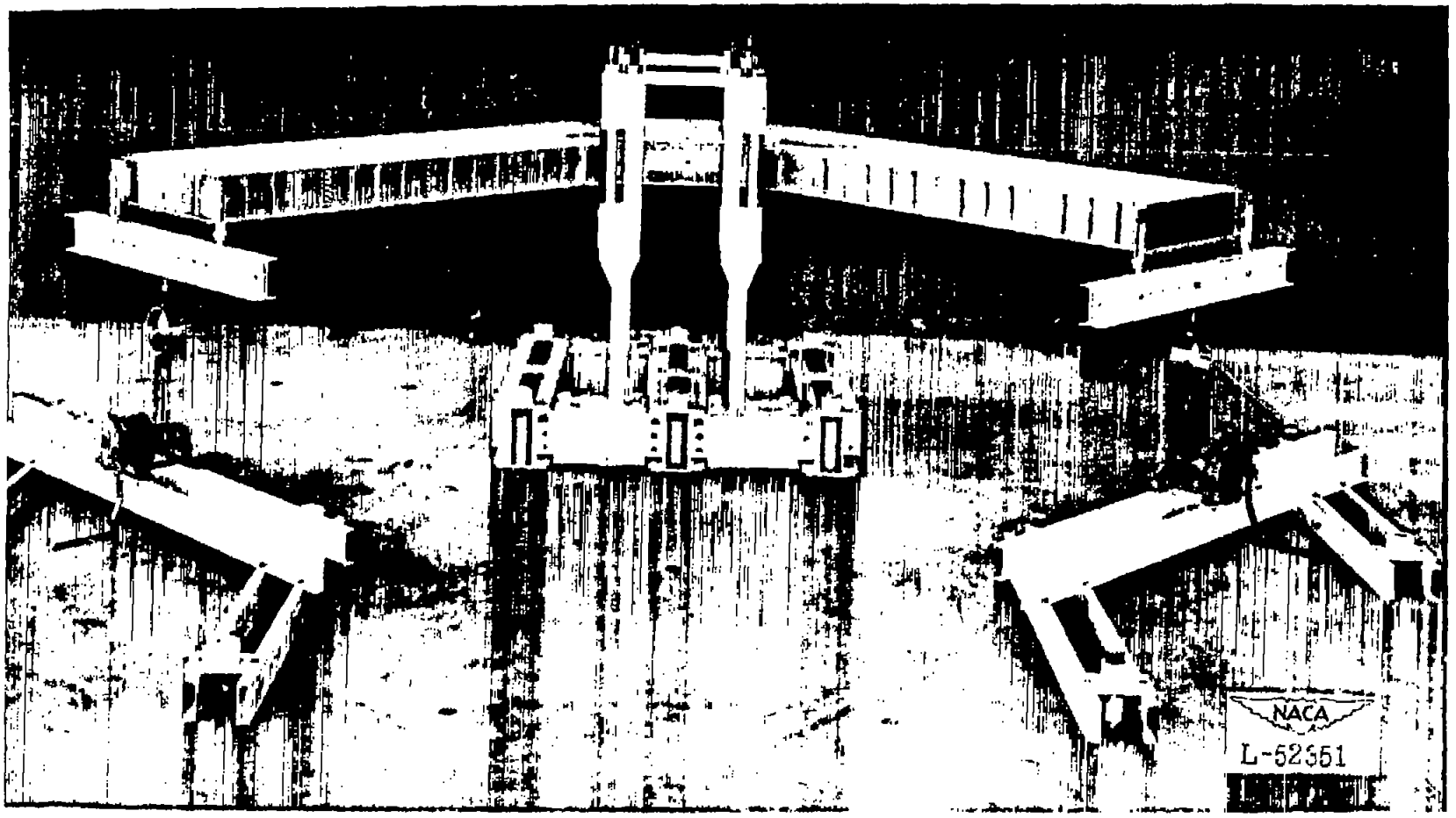

Figure 1.- Bending test setup of sweptback box beam.

NATIONAL ADVISORY COMMITTEE FOR AERONAUTICS
LANGLEY MEMORIAL AERONAUTICAL LABORATORY - LANGLEY FIELD VA

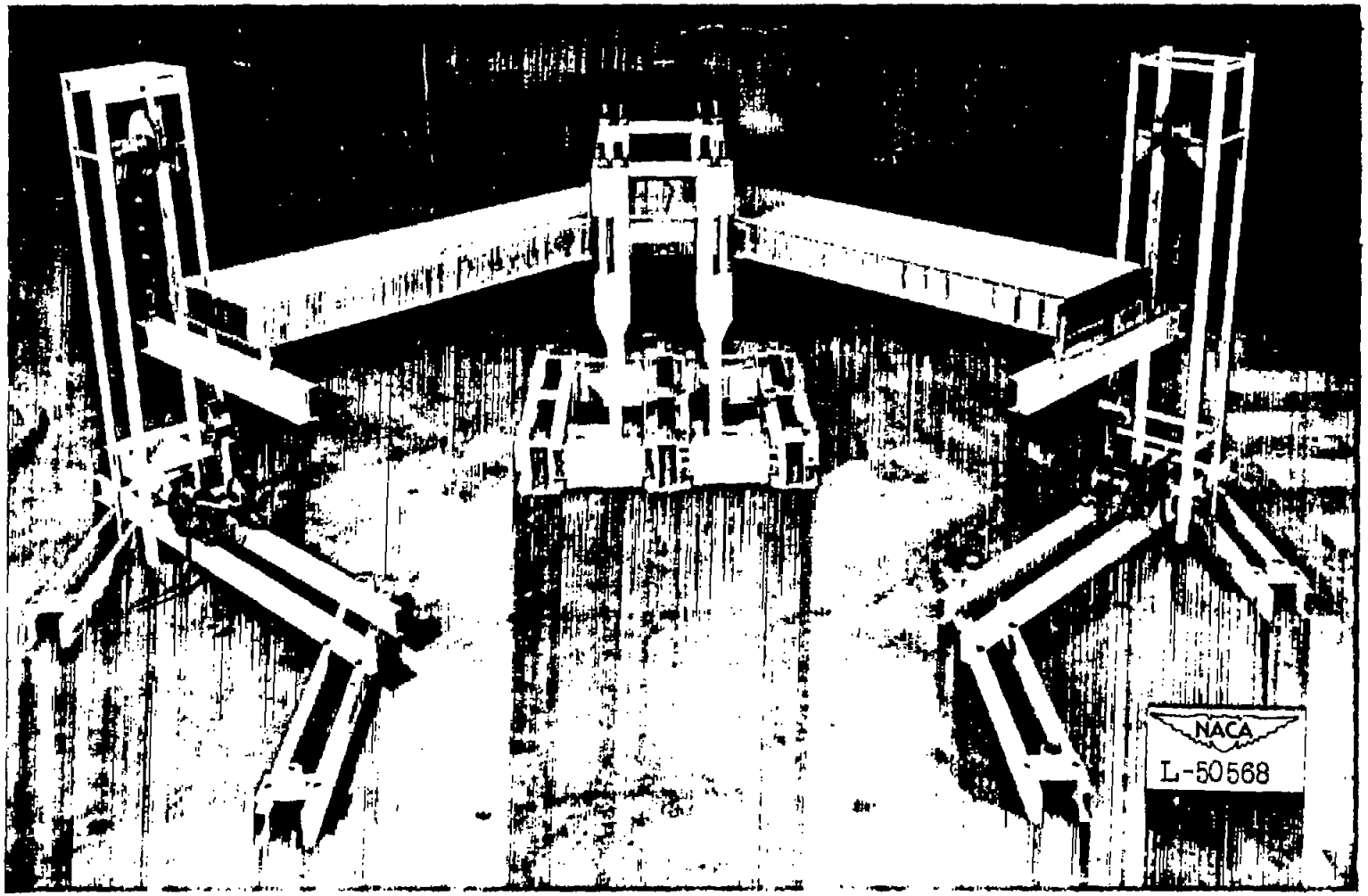

Figure 2.- Torsion test setup of sweptback box beam.

NATIONAL ADVISORY COMMITTEE FOR AERONAUTICS
LANGLEY MEMORIAL AERONAUTICAL LABORATORY - LANGLEY FIELD VA

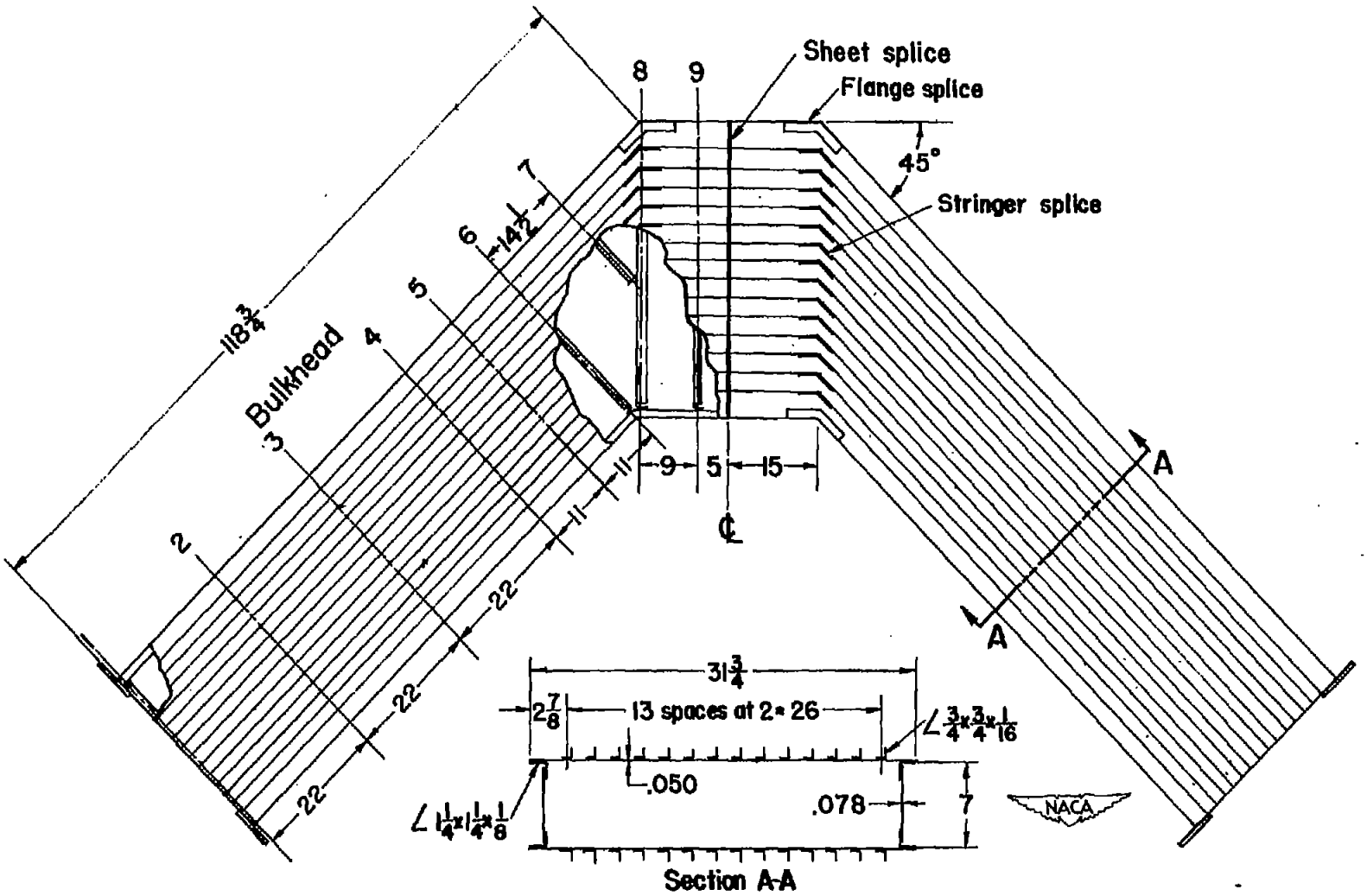

Figure 3.- Details of sweptback box beam.

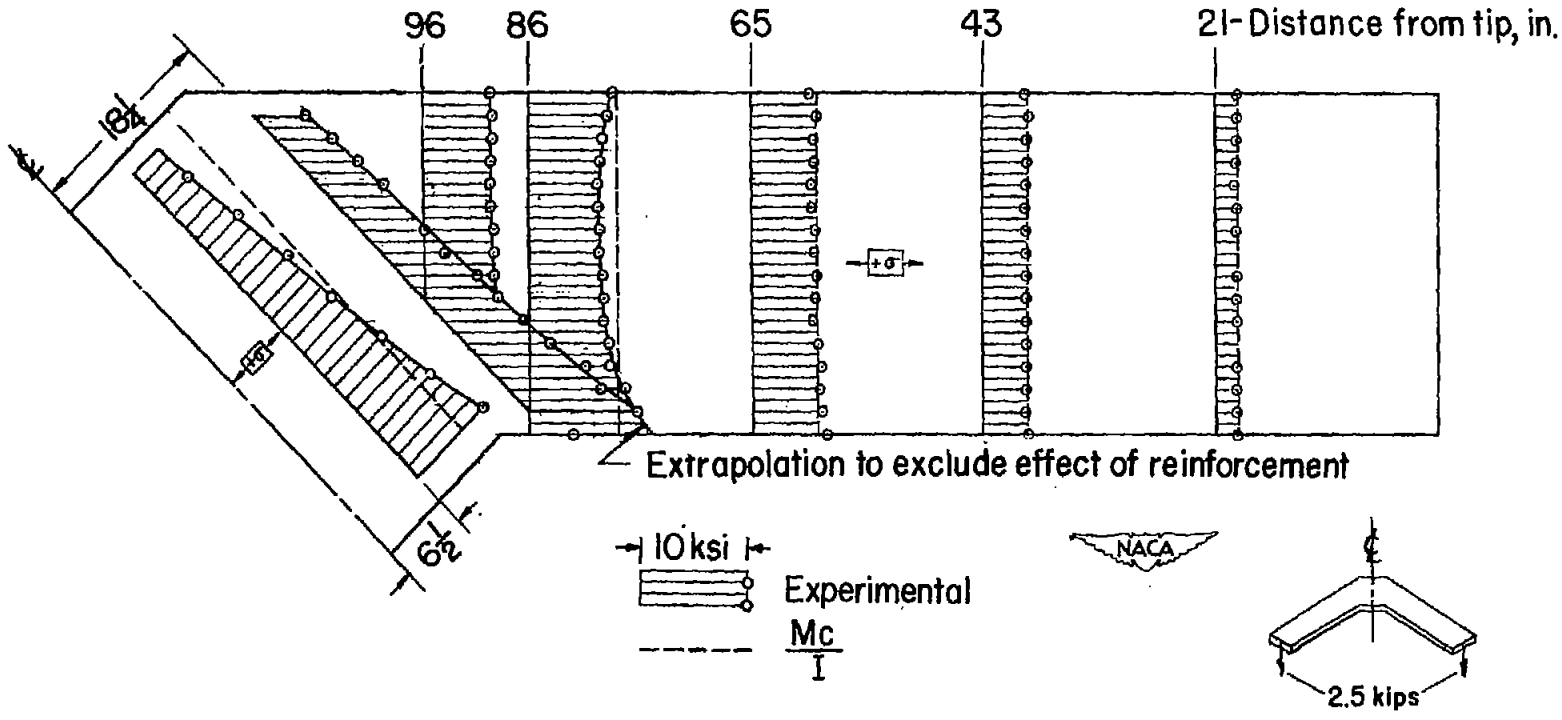

Figure 4.- Stringer and flange stresses of sweptback box beam for tip bending load.

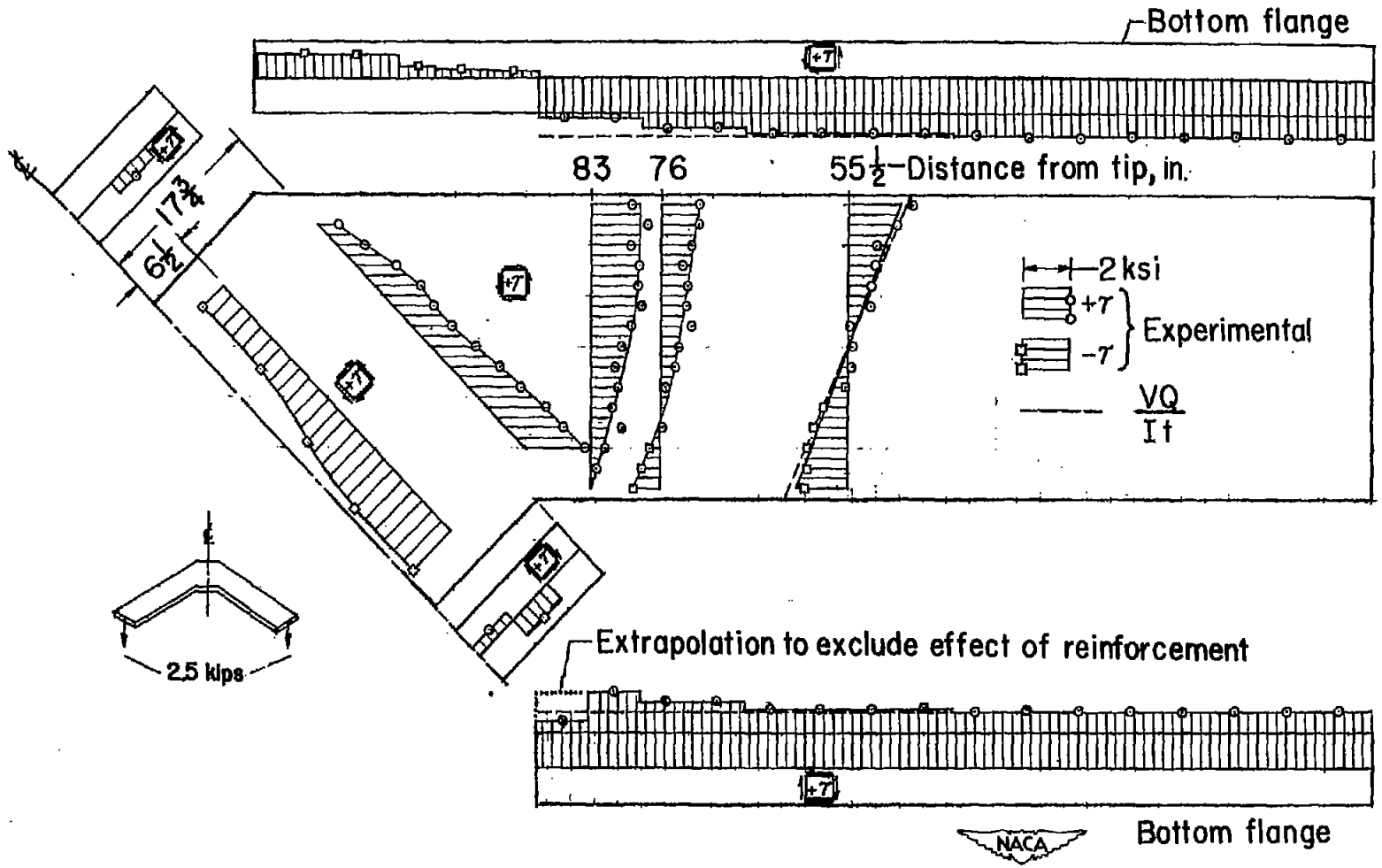

Figure 5.- Shear stresses in top cover and spar webs of sweptback box beam for tip bending load.

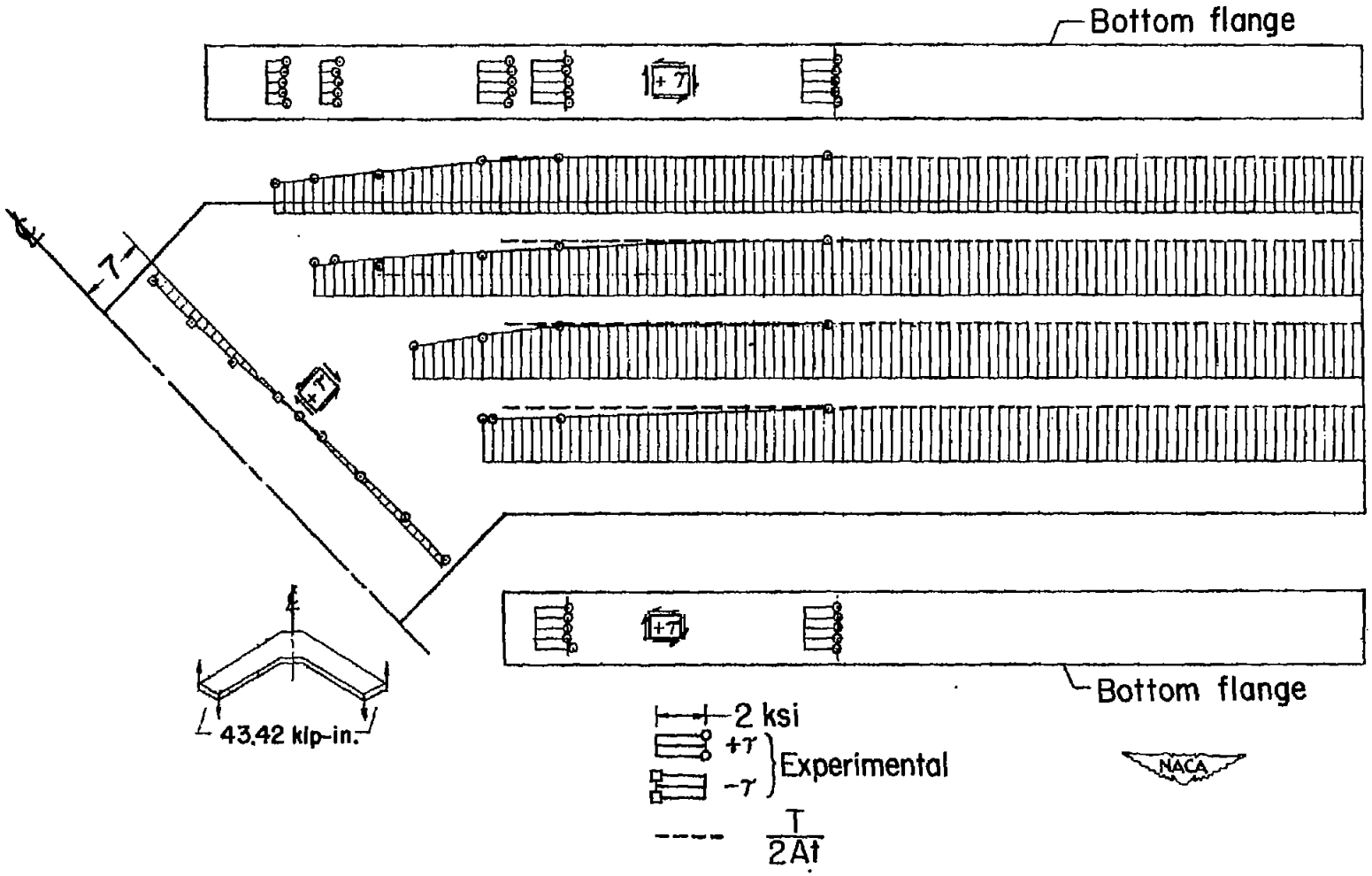

Figure 6.- Shear stresses in top cover and spar webs of sweptback box beam for tip torque.

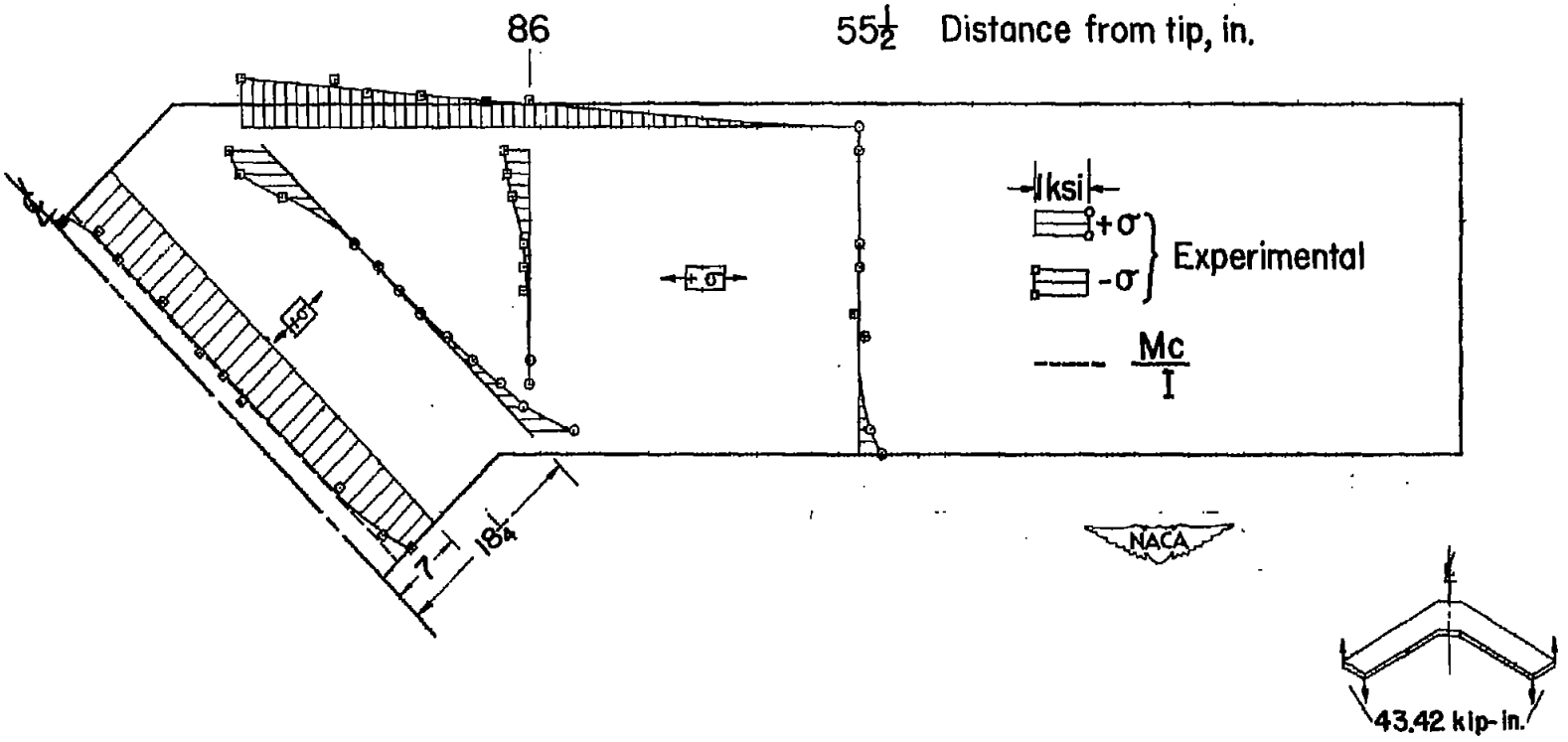

Figure 7.- Stringer and flange stresses of sweptback box beam for tip torque.

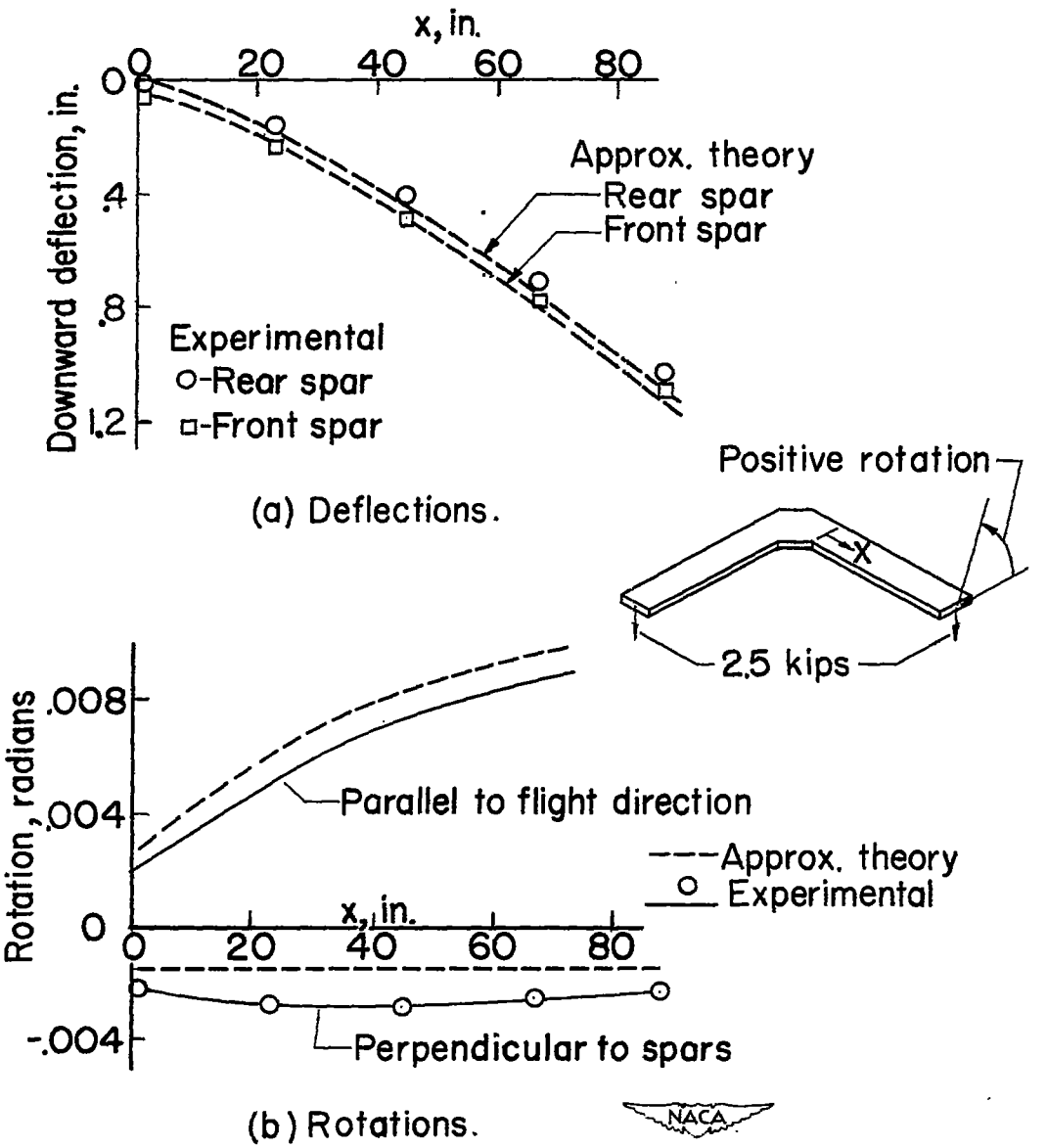

Figure 8.- Distortions of sweptback box beam for tip bending load.

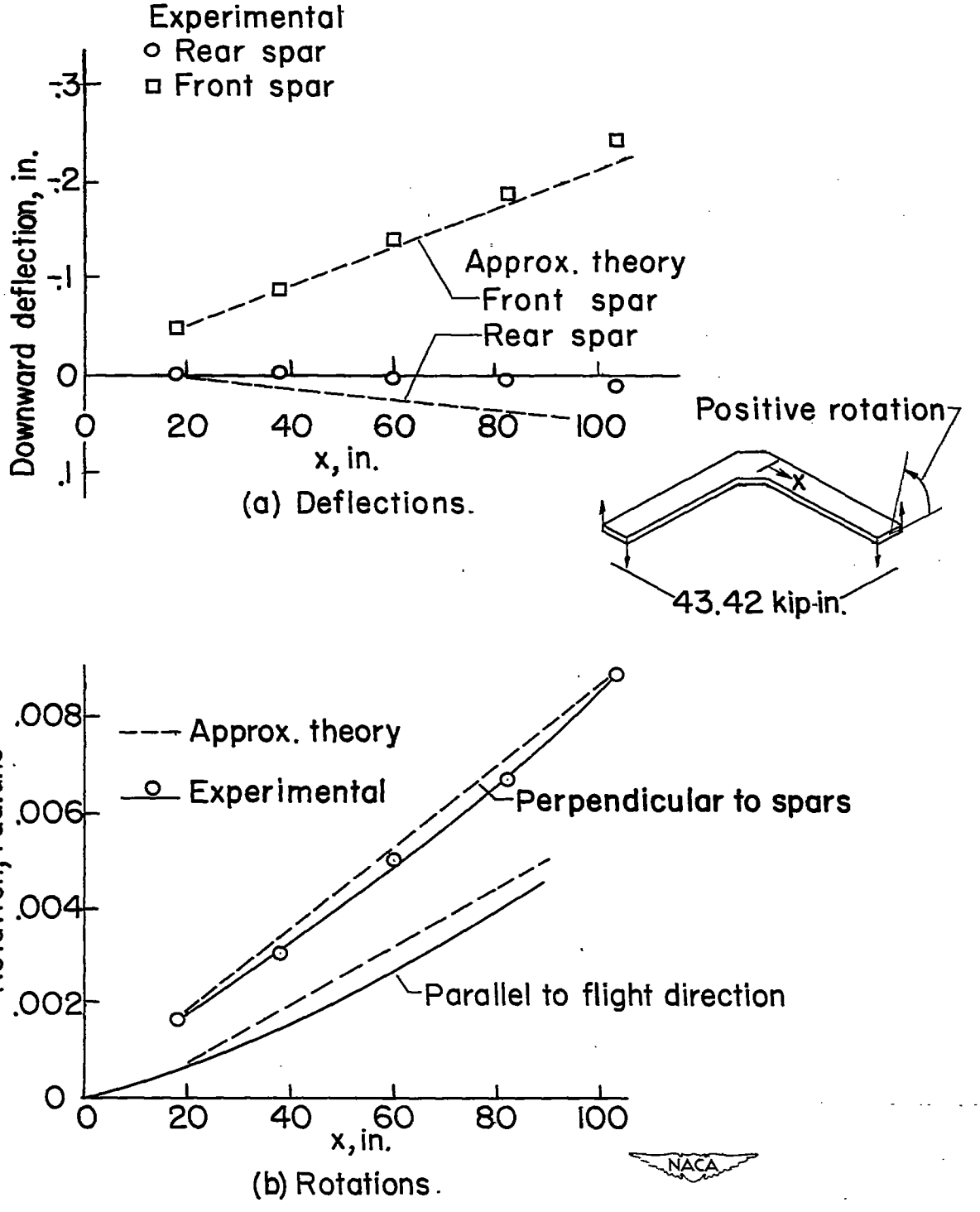

Figure 9.- Distortions of sweptback box beam for tip torque.

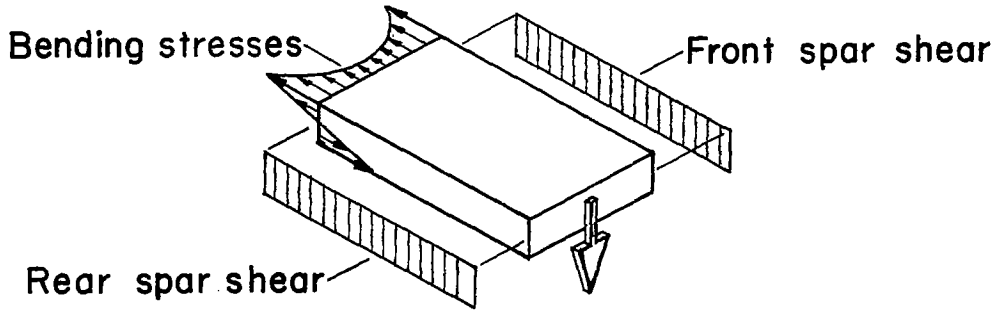

(a) Stress distributions for symmetrical restraint at cantilever root.

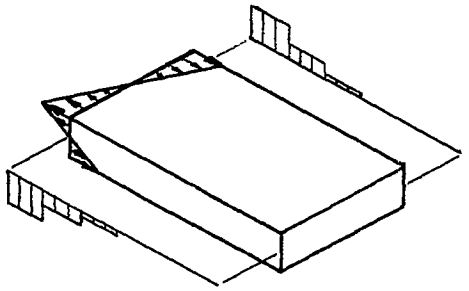

(b) Stress distribution to produce warping of root cross section.

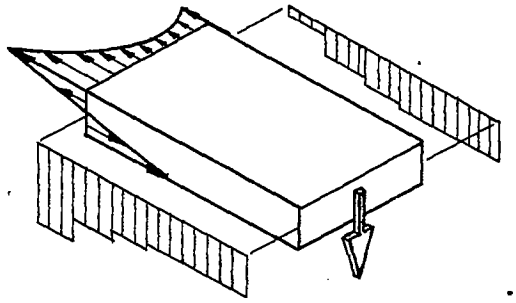

(c) Stress distribution in cantilever portion of sweptback box beam, obtained by superposition of (a) and (b).

Figure 10.- Qualitative stress distribution in cantilever portion of sweptback box beam, obtained by superposition.